Effect of Silk Fibroin Interpenetrating Networks on Swelling/Deswelling Kinetics and Rheological Properties of Poly(*N*-isopropylacrylamide) Hydrogels

Eun Seok Gil† and Samuel M. Hudson*

Fiber and Polymer Science Program, North Carolina State University, Raleigh, North Carolina 27695

Received June 7, 2006; Revised Manuscript Received September 13, 2006

Novel protein/synthetic polymer hybrid interpenetrating polymer networks (IPNs) of poly(*N*-isopropylacrylamide) (PNIPAAm) with *Bombyx mori* silk fibroin (SF) have been prepared by using methanol to postinduce SF crystallization. Those IPNs having the β sheet crystalline structure of SF show improved storage and loss moduli. The IPN hydrogels show the same volume phase transition temperature and NaCl concentration as pure PNIPAAm hydrogels. The PNIPAAm/SF IPNs keep the swelling kinetics of PNIPAAm, while showing increased deswelling kinetics. The IPNs with SF β sheet structure should decrease the formation of the skin layer observed in conventional PNIPAAm hydrogels. Therefore, the proposed IPN hydrogels composed of protein/polymer provide fast deswelling rates as well as improved mechanical properties over pure PNIPAAm hydrogels. The effect of SF β sheet networks on the IPNs copolymerized with acrylic acid (AAc) (P(NIPAAm-*co*-AAc)/SF IPNs) is compared with that on the PNIPAAm/SF IPNs, and the parameters controlling the deswelling kinetics of the IPNs are investigated. Three parameters, (1) the skin layer formation, (2) the restriction of SF β sheet networks, and (3) the aggregation force of NIPAAm chains, are cooperatively involved in the deswelling process of IPN hydrogels according to the SF content and the presence of the AAc moiety.

Introduction

Stimulus-responsive polymers have been vigorously investigated due to their attractive properties: they undergo relatively large and abrupt, physical or chemical changes in response to small external changes in the environmental conditions. These polymer systems have been utilized in biorelated applications such as drug delivery[1−3] and biotechnology.[4−5] Recently we reported a systematic review of the molecular designs of stimulus-responsive polymers according to the types of responding stimuli and physical forms with their biorelated applications.[6] Stimulus-responsive polymers can be applied in different forms as follows: cross-linked (permanently) hydrogels,[7−9] thermoreversible hydrogels,[10,11] micelles,[12] modified interfaces,[13,14] and conjugated solutions.[15] Among these physical forms, hydrogels, which are formed with a three-dimensional (e.g., chemically or physically cross-linked) network of hydrophilic polymer chains, swell, but do not dissolve in an aqueous environment.

Poly(*N*-isopropylacrylamide) (PNIPAAm) has been the most actively investigated temperature-responsive polymer due to its sharp phase transition (a lower critical solution temperature (LCST)) in water at around 32 °C.[16] The limitations to hydrogels composed of PNIPAAm have been discussed, such as biocompatibility, deswelling rate, and mechanical properties.[6] The need to improve these properties led to the introduction of other functionalities. The PNIPAAm-based hydrogels have been modified to be more versatile materials by incorporating more hydrophilic moieties in the polymer backbone or the graft chain[17,18] and by introducing interpenetrating polymer networks (IPNs).[19,20]

PNIPAAm hydrogels have a very slow deswelling rate due to the formation of a skin layer, which interrupts the release of internal water molecules in the deswelling process. The modification of hydrogels on the microstructure scale could lead to a shorter response time to stimuli.[21] Chemical modification of PNIPAAm networks, such as copolymerization with acrylic acid (AAc)[7] and incorporation of graft chains with PNIPAAm[9] or poly(ethylene oxide) (PEO),[17] has been reported to accelerate the deswelling kinetics by suppressing the formation of the skin layer. IPNs of PNIPAAm were introduced to improve the deswelling rate.[22]

Silk fibroin (SF), which can be obtained by degumming silkworm silk from *Bombyx mori*, is a fibrous protein of silk fiber and consists of heavy (350 kDa) and light (25 kDa) chain polypeptides, connected by a disulfide link.[23,24] The heavy chain consists of a high content of Gly-Ala-Gly-Ala-Ser repeats constructing β sheet structures in the fibrous form.[23] The regenerated fiber[25] and scaffold[26] have been introduced for biomaterials due to good mechanical strength in the wet state,[26] biocompatibility for the growth of cells,[27] high dissolved oxygen and water vapor permeability,[28] and resistance against enzymatic degradation.[29] It has been shown that silk fibroin films cast from aqueous solution are mainly in the amorphous state.[25] Our previous report described the solvent-induced SF β sheet crystalline structure in a blend hydrogel system with another protein biopolymer, gelatin.[30−32]

In this study, interpenetrating polymer networks (IPNs) of PNIPAA and SF are synthesized and examined, anticipating higher mechanical strength and accelerated deswelling kinetics by suppressing the skin layer formation. The volume phase transition behaviors of PNIPAAm/SF IPN hydrogels according to the temperature and salt concentration are compared with those of pure PNIPAAm hydrogels. Also, the effects of SF β-sheet crystalline networks on the viscoelastic properties and swelling/deswelling properties are investigated. The hydrophilic AAc moiety was incorporated in PNIPAAm backbones. P(NIPAAm-*co*-AAc)/SF IPNs were synthesized and compared

* To whom correspondence should be addressed. E-mail: Sam_Hudson@ncsu.edu.

† Present address: Department of Surgery, Pennsylvania State University, Hershey, PA 17033.

10.1021/bm060543m CCC: $37.00
Published on Web 11/24/2006

Scheme 1. Illustration of the PN/SF and PNA/SF IPN Hydrogels as They Respond to a Temperature Change in an Aqueous Environment[a]

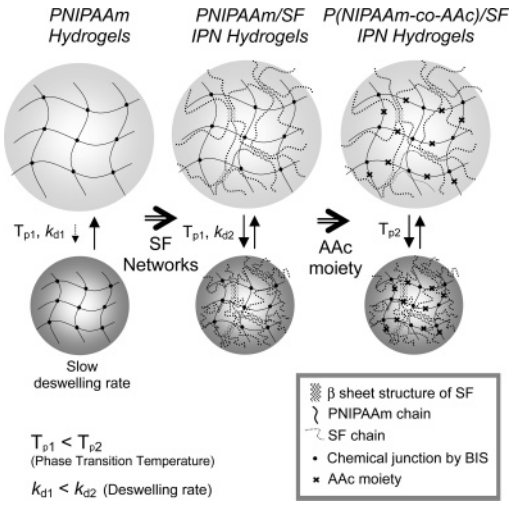

[a] The PNIPAAm networks undergo expansion/aggregation responding to temperature, while the β sheet structure of SF remains intact and enhances the mechanical properties of the hydrogel network. Incorporation of AAc increases the phase transition temperature (T_p) and swelling ratio of the IPN hydrogels. However, SF networks do not change the T_p of PNIPAAm and PNIPAAm-*co*-AAc hydrogels. The β sheet structure of SF reduces the skin layer effect, resulting in a faster deswelling rate than that of the pure PNIPAAm hydrogel.

with PNIPAAm/SF IPNs. From the change of the deswelling kinetics with the SF content and AAc moiety in the IPN hydrogels, we elucidated the parameters controlling the deswelling kinetics of the IPN hydrogels. Their schematic structure and temperature-responsive nature are illustrated in Scheme 1.

Experimental Section

Materials. NIPAAm (Aldrich Chemical Co., Milwaukee) was recrystallized twice from *n*-hexane. AAc (Aldrich) was purified by distillation at 55 °C in high vacuum. *N*,*N*′-Methylenebis(acrylamide) (BIS), ammonium persulfate (APS), *N*,*N*,*N*′,*N*′-tetramethylethylenediamine (TEMED), sodium lauryl sulfate, sodium carbonate, PEO (M_v = ca. 600000, Aldrich), and calcium nitrate were purchased from Aldrich or Fisher and used as received. Grade 5A raw silk with an average denier of 20.86 produced in Brazil by the Fiaçào de Seda Bratac S.S. was used. All chemicals were of analytical grade. Phosphate-buffered saline solution (PBS; pH 7.4) was used for all the experiments.

Methods. *Preparations.* The *B. mori* silk was degummed with 0.25% (w/v) sodium lauryl sulfate and 0.25% (w/v) sodium carbonate in boiling water, bath ratio of 1:10 (w/v), for 1 h. The dried silk fibroin (20 g) was dissolved in $Ca(NO_3)_2 \cdot 4H_2O$/MeOH (75:25, w/w) solution (180 g) at 67 °C for 6 h. The silk fibroin solution (10%, w/w) was dialyzed with a cellulose membrane tube (MWCO = 6000−8000) for 4 days by changing the deionized water daily.[25] The concentration of the dialyzed SF solution was controlled to 10% (w/v) by dialyzing reversely with PEO powder.

NIPAAm and SF blend solutions were prepared to a final total concentration of 10% (w/v) by mixing an aqueous NIPAAm (10%, w/v) and SF (10%, w/v) solution. Also, an aqueous monomer mixture solution (10% w/v of monomers) of NIPAAm (98.7 wt %) and AAc (1.3 wt %) was prepared and then blended with an SF (10% w/v) solution according to the desired blending ratios. A 1.3 wt % AAc-containing PNIPAAm hydrogel has been reported to show a maximum deswelling rate, since the AAc segments suppressed the skin layer effect, but also interrupted the long linear NIPAAm segments over the higher content of the AAc moiety, resulting in their decreased hydrophobic aggregation forces.[17] The deswelling rate rebounded over a certain threshold of AAc content (over 1.3 wt %), enough to suppress skin layer formation. Therefore, 1.3 wt % AAc to PNIPAAm was selected to investigate the effect of the SF crystalline structure on the AAc-containing PNIPAAm hydrogels with rapid deswelling kinetics. The composition of each PNIPAAm/SF (PN/SF) or P(NIPAAm-*co*-AAc)/SF (PNA/SF) hydrogel, denoted by PN/SF*W* or PNA/SF*W* (where *W* denotes the weight percent of PN or PNA), was controlled by mixing predetermined quantities of the parent solutions. PN/SF and PNA/SF IPN hydrogels were prepared by free radical polymerization of NIPAAm and additional organic solvent treatment to induce a β sheet crystalline network of SF. BIS (2.7 wt % (2.0 mol %) NIPAAm) as a cross-linker and TEMED (10 μL) as an accelerator were additionally dissolved in 10 mL of NIPAAm/SF solution, and dry argon gas was bubbled into the solution for 10 min to remove the dissolved oxygen. After APS (10 mg) as an initiator was added, the solution was thoroughly stirred, immediately poured into a glass mold (3 mm thick), and covered with a glass plate. The solution mixture was polymerized at 10 °C for 1 day. The gel membrane which formed was immersed in methanol (gel weight:methanol = 1:3 (w/w)) for 1 day to introduce the β sheet conformation of SF into the PNIPAAm networks and dried in air for 2 days. The dried membrane was immersed in pure water at ambient temperature for 7 days by changing the pure water daily to remove unreacted chemicals. The swollen IPN hydrogels were cut into disks (12 mm diameter) with a cork borer. The disk-type gels were dried in air for 2 days and additionally dried in a vacuum for 1 day.

Analysis. The wide-angle X-ray diffraction (WAXD) curve of the PNIPAAm/SF film was obtained with a Seimens type F X-ray diffractometer. Ni-filtered Cu Kα radiation was used for the X-ray source at 35 kV and 25 mA. All scans were performed from 5° to 40° (2θ) at a speed of 1.0 deg/min. We investigated the viscoelastic properties of PNIPAAm/SF semi-IPN (before MeOH treatment) and IPN (after MeOH treatment) hydrogels by dynamic shear oscillation measurements at small constant shear strain. We carried these measurements out with a REOLOGICA rheometer (REOLOGICA Instruments AB) using parallel plates of 25 mm diameter. The loaded normal force onto each hydrogel film was automatically adjusted at 2.0 N. We measured the mechanical spectra with a constant shear strain of 0.1% over a frequency range of 0.1−10 Hz at 17 °C.

The swelling ratios of the hydrogel samples were gravimetrically monitored as a function of composition (PNIPAAm to SF) in the temperature range from 20 to 45 °C and NaCl concentration range from 0 to ~4 M. The experimental plots were obtained from averages of three samples. The equilibrium swelling ratio was defined as the weight of absorbed water (W_w) per weight of the dried gel (W_g). The water content is defined as $(W_w/W_h) \times 100$, where W_h is the weight of the hydrogel. For a dynamic swelling kinetic study, the hydrogels were swollen in PBS (pH 7.4) at 20 and 45 °C, removed, wiped with moistened tissue paper, and weighted at regular intervals. For a temperature dependence study on swelling ratios, the swelling ratios of the IPN hydrogels were monitored by lowering the temperature stepwise from 45 to 20 °C after at least a 2 day soaking at each targeted temperature. The desired temperature was controlled by a thermostated water bath (Precision digital water bath) with a resolution of ±0.05 °C.

To measure the deswelling kinetics, the IPN hydrogles were equilibrated in PBS at 20 °C and quickly transferred into PBS at 45 °C. The IPN hydrogels were taken out of PBS at regular intervals and weighed after removal of excess water from the IPN hydrogel surface. The deswelling kinetics were defined by the temperature-dependent weight changes of the IPN gels and were illustrated between equilibrium swollen (100%) states at 20 °C and equilibrium shrunken (0%) states at 45 °C. The initial deswelling rate of the hydrogels was calculated from the weight decreases of the hydrogels for the initial 5 min and defined as the decreased gel weight per 5 min per swollen gel weight at 20 °C per 5 min [(g/g)/min].

For the measurement of the oscillating swelling/deswelling kinetics of the IPN hydrogels in response to a temperature jump, the IPN

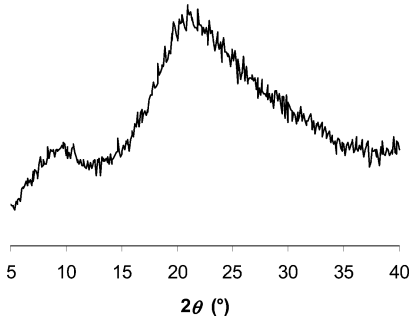

Figure 1. WAXD curve of PNIPAAm/SF (40/60) (PN/SF40) IPNs.

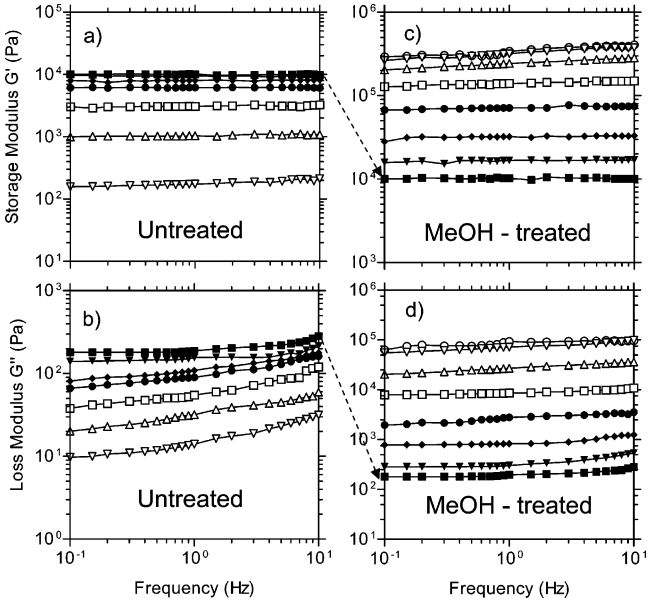

Figure 2. Frequency dependence of the dynamic storage and loss moduli of PN/SF hydrogels differing in composition (*W*, wt % PN): 100 (■), 90 (▼), 80 (◆), 70 (●), 60 (□), 40 (△), 20 (▽), 0 (○); (a, b) untreated PN/SF, (c, d) treated PN/SF under the experimental conditions described in the text.

hydrogels were rapidly transferred between 20 and 45 °C PBS solution over 4 min temperature cycles. The IPN hydrogels were taken out, wiped with moistened tissue paper, and weighed at regular intervals.

Results and Discussion

SF Structure in PNIPAAm Networks. To investigate the induced β sheet crystalline structure of SF in PNIPAAm networks, WAXD was used. Figure 1 shows the WAXD curves of a PN/SF40 dried film after the methanol treatment as described above. It was reported that a broad peak is shown at $2\theta = 20°$ in regenerated SF as a typical characteristic pattern of an amorphous structure, and a major peak is observed at $2\theta = 21°$ and two minor peaks at 9° and 24° in a methanol-treated SF, assigned as characteristic peaks of a β sheet crystalline structure.[25] The treated PN/SF shows a strong peak at $2\theta = 21°$, indicating that a β sheet conformation of SF was induced in the PNIPAAm networks. This result supports that the β sheet crystalline structure of SF is successfully introduced into the PNIPAAm networks and that the PNIPAAm networks interrupt little, if any, the conformational change of SF by increased topological constraints such as entanglements.

Rheological Study of IPN Hydrogels. Figure 2 shows the storage modulus (G') and loss modulus (G'') of the PN/SF hydrogels as a function of frequency at 17 °C. In these mechanical spectra, G' is considerably higher than G'' in all

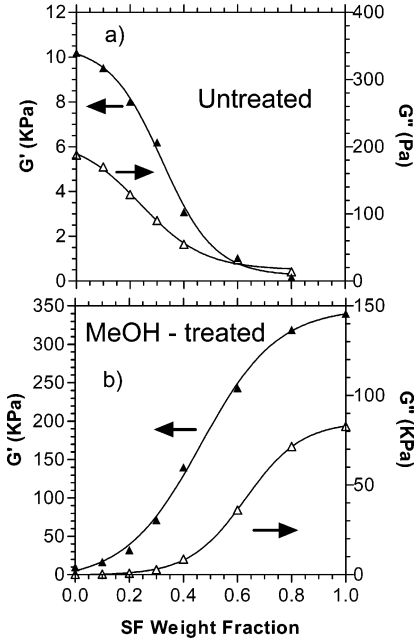

Figure 3. Discrete values of G' (▲) and G'' (△) of PN/SF hydrogels at a frequency of 1 Hz: (a) untreated PN/SF hydrogels, (b) treated PN/SF hydrogels. The solid lines correspond to curve fits of the Bolzmann sigmoidal expression.

compositions of PNIPAAm and silk fibroin, which means that the hydrogels represent typical characteristics of well-developed polymeric networks. The PN/SF hydrogels, prepared without methanol treatment, show lower G' and G'' with a higher content of SF. These SF chains only contribute amorphous structure without physical cross-links in the PNIPAAm networks.

These complex hydrogels represent a semi-IPN structure. The gel network density of PNIPAAm should be lower with a higher content of SF, so the moduli of complex hydrogels would be lower than those of a pure PN/SF100 hydrogel. By contrast, the methanol treatment leads the PN/SF hydrogels to show a fully developed IPN structure as shown in the X-ray result, resulting in increased viscoelastic properties with more SF content. Interestingly, the order of the moduli increases from a lower content of SF to a higher content of SF, which is opposite the tendency of the untreated complex hydrogels, because the untreated ones showed lower moduli with a higher content of SF.

Figure 3 represents the discrete values of G' and G'' of the IPN hydrogels selected at a frequency of 1 Hz. Both G' and G'' of the untreated PN/SF hydrogels decrease with more SF content, exhibiting a sigmoidal dependence on the hydrogel composition. However, G' and G'' of the treated PN/SF hydrogels increase with more SF weight fraction, showing likewise a sigmoidal dependence on the hydrogel composition. This indicates that the β sheet crystalline structure of SF in the PN/SF IPN hydrogels enhanced the viscoelastic properties of the PNIPAAm networks. One drawback of the PNIPAAm hydrogel has been its physical properties in the gel state.

Swelling Behaviors of IPN Hydrogels. Figure 4 shows the dynamic swelling of the PN/SF and PNA/SF IPN hydrogels in PBS (pH 7.4) at 20 and 45 °C. The swelling data (Q) in this and subsequent figures can be represented by a general kinetic expression of the form

$$Q = A + \frac{k_1 t}{1 + k_2 t} \qquad (1)$$

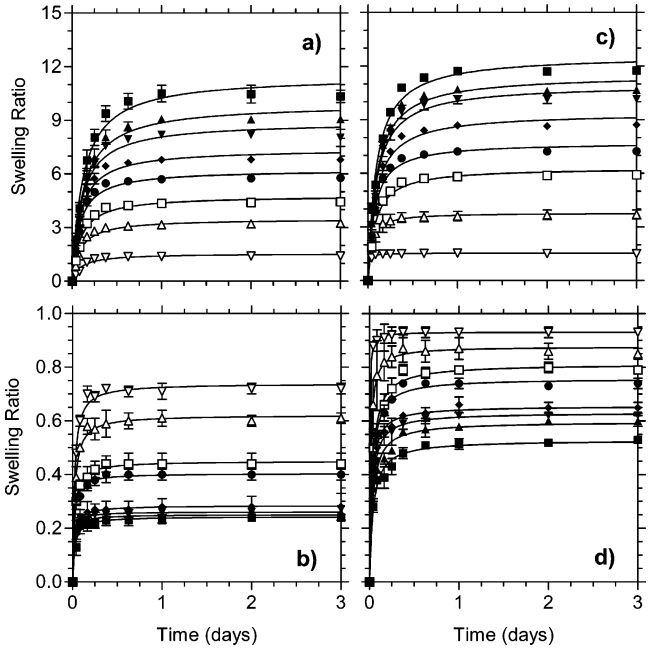

Figure 4. Dynamic swelling curves of IPN hydrogels differing in composition (*W*, wt % PN or PNA) in PBS (pH 7.4): 100 (■), 95 (▲), 90 (▼), 80 (◆), 70 (●), 60 (□), 40 (△), 20 (▽); PN/SF hydrogels (a) at 20 °C and (b) at 45 °C; PNA/SF hydrogels (c) at 20 °C and (d) at 45 °C. The error bars denote the standard error ($N = 3$). The solid lines correspond to regressions of eq 1 to the data. Values of parameters acquired from these regressions are listed in Tables 1 and 2.

Table 1. Kinetic Parameters Discerned by Regression Analysis of the PN/SF Hydrogel Swelling Data

temp (°C)	*W* (wt % PN)	*A*	k_1 (days^{-1})	k_2 (days^{-1})	Q_∞[a]
20	100	0.00	94.9	8.27	11.5
	95	0.00	82.9	8.35	9.93
	90	0.00	85.1	9.54	8.92
	80	0.00	80.5	10.9	7.41
	70	0.00	74.6	12.0	6.24
	60	0.00	49.3	10.4	4.80
	40	0.00	38.6	11.1	3.48
	20	0.00	16.0	10.3	1.55
45	100	0.00	10.1	41.7	0.243
	95	0.00	15.9	63.3	0.251
	90	0.00	21.4	81.8	0.261
	80	0.00	14.5	50.9	0.284
	70	0.00	26.1	64.5	0.404
	60	0.00	21.6	47.9	0.450
	40	0.00	28.4	45.7	0.622
	20	0.00	37.4	50.6	0.739

[a] Calculated from $A + k_1/k_2$.

where A, k_1, and k_2 are fitting parameters. If Q is considered as 0 at $t = 0$, A is 0. Values of the fitting parameters extracted from the data in Figure 4 via nonlinear regression analysis are listed in Tables 1 and 2. Also, values of long-time swelling discerned from regression of eq 1 to the data (Q_∞) were calculated from $A + k_1/k_2$.

At 20 °C, below the phase transition temperature (T_p), the IPN hydrogels with the higher content of SF show lower swelling ratios. However, all IPN hydrogels reach an equilibrium state within 1 day, showing swelling kinetics similar to those of the PN/SF100 (or PNA/SF100) hydrogel. At 45 °C, above the T_p, the swelling ratios of the IPN hydrogels are very low, but the order of the swelling ratios (Q_∞ values in Tables 1 and 2) according to the SF content is totally opposite that of the swelling ratios at 20 °C. This means that the shrunken conformation of PNIPAAm (or P(NIPAAm-*co*-AAc)) networks above the T_p provides a more repulsive force for dehydration than even very fine β sheet crystalline networks of SF. All IPN hydrogels reach equilibrium swelling within 9 h. The incorporation of an AAc moiety into the PNIPAAm networks increased the swelling ratios of the PN/SF IPN hydrogels (see the Q_∞ values in Table 2) in all compositions at 20 °C as well as 45 °C, since the hydrophilic moiety (AAc) should tend to retain a larger amount of water.

Table 2. Kinetic Parameters Discerned by Regression Analysis of the PNA/SF Hydrogel Swelling Data

temp (°C)	*W* (wt % PN)	*A*	k_1 (days^{-1})	k_2 (days^{-1})	Q_∞[a]
20	100	0.00	137	10.9	12.6
	95	0.00	123	10.6	11.5
	90	0.00	120	11.0	11.0
	80	0.00	105	11.2	9.38
	70	0.00	108	14.0	7.74
	60	0.00	78.5	12.4	6.31
	40	0.00	104	27.4	3.78
	20	0.00	213	138	1.54
45	100	0.00	13.2	25.0	0.529
	95	0.00	16.9	28.2	0.597
	90	0.00	22.4	35.5	0.631
	80	0.00	27.0	41.1	0.656
	70	0.00	26.5	34.9	0.759
	60	0.00	26.0	32.0	0.812
	40	0.00	68.9	78.5	0.877
	20	0.00	359	386	0.931

[a] Calculated from $A + k_1/k_2$.

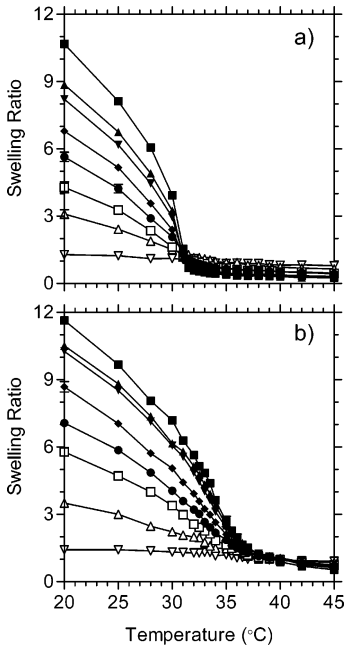

Figure 5. Equilibrium swelling ratios for (a) PN/SF and (b) PNA/SF IPN hydrogels differing in composition (*W*, wt % PN or PNA) in PBS (pH 7.4) in the temperature range from 45 to 20 °C: 100 (■), 95 (▲), 90 (▼), 80 (◆), 70 (●), 60 (□), 40 (△), 20 (▽). The solid lines serve to connect the data, and the error bars, which are smaller than the symbols employed here, denote the standard error ($N = 3$).

Figure 5 shows equilibrium swelling ratios for PN/SF IPN (a) and PNA/SF IPN (b) hydrogels in PBS (pH 7.4) in the temperature range from 45 to 20 °C. The IPN hydrogels are

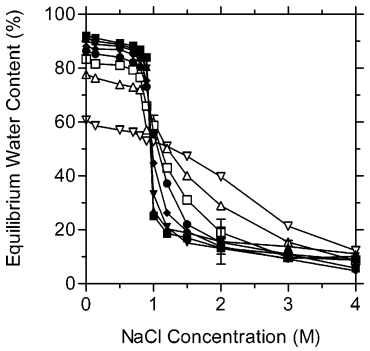

Figure 6. Effect of the NaCl concentration on the water content of the PN/SF IPN hydrogels differing in composition (*W*, wt % PN): 100 (■), 95 (▲), 90 (▼), 80 (◆), 70 (●), 60 (□), 40 (△), 20 (▽). The solid lines serve to connect the data, and the error bars, which are smaller than the symbols employed here, denote the standard error ($N = 3$).

swollen at lower temperature than the T_p and shrunken above the T_p. In general, the LCST of a temperature-responsive polymer is known to be influenced by hydrophobic or hydrophilic comonomers in its molecular chains. Copolymerization with a small ratio of hydrophilic monomers, such as acrylamide and acrylic acid,[33] has been reported to increase T_p to higher temperature as well as their swelling properties. The more hydrophilic moiety in PNIPAAm chain would make the LCST increase and even disappear.[34] The T_p values of PN/SF IPN and PNA/SF IPN hydrogels are observed respectively at 31 and 37 °C, at which pure PN/SF100 and pure PNA/SF100 hydrogels also show their T_p values, respectively. This indicates that SF crystalline networks interfere rarely, if any, with the forces triggering conformational changes of PNIPAAm, even though the amount of water absorbed into the IPN networks is changed by the SF crystalline structure. The fact that the entanglement does not change the T_p implies that the molecular interaction of PNIPAAm operates at a smaller scale than the entanglement lengths. However, PN/SF20 shows a small and gradual increase of swelling without significant phase transition behavior. This indicates that a too high content of SF might suppress abrupt hydration caused by a conformational change of the PNIPAAm molecules.

Salt Effects on the Phase Transition of IPN Hydrogels. PNIPAAm has been investigated not only for its temperature-responsive phase transition but also for its salt-responsive phase transition.[20] Usually, the salt effect on hydrogels has been reported for polyelectrolyte polymers such as a block copolymer composed of *N*,*N*′-dimethylaminoethyl methacrylate (DMAEMA).[35] However, it is interesting that nonionic PNIPAAm hydrogels show a volume phase transition responding to the salt concentration. Pack et al. explained that the chloride ion plays a role to induce dehydration of the hydrogels by the mechanism of interfering with the bound water around the PNIPAAm chains.[36] Dhara et al. report that PNIPAAm hydrogels in IPNs with gelatin exhibit phase transition at the same salt concentration as pure PNIPAAm hydrogels without hindering the dehydration of the PNIPAAm chains by the more hydrophilic characteristic of gelatin.[20] In the case of our PN/SF IPNs, fine SF β sheet crystalline networks might disrupt the salt effect on the PNIPAAm chains. Therefore, the effect of the NaCl concentration on the water content of the PN/SF IPN hydrogels remains to be investigated to reveal this supposition and is represented in Figure 6. The IPN hydrogels abruptly shrink above 1.0 M NaCl, but the slope of the phase transition becomes lower with more SF content, and even PN/SF20 does not show an abrupt phase transition at 1.0 M NaCl

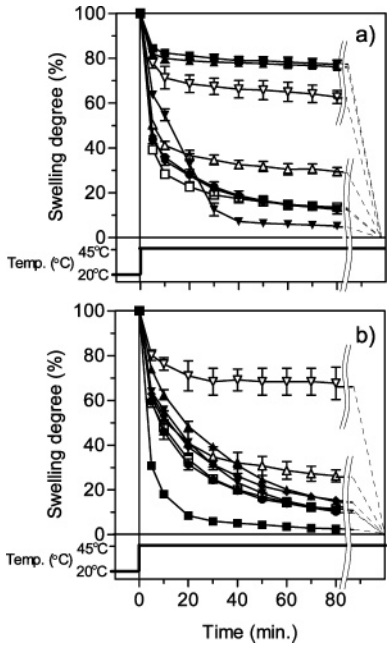

Figure 7. Deswelling kinetics of (a) PN/SF and (b) PNA/SF IPN hydrogels differing in composition (*W*, wt % PN or PNA) in PBS (pH 7.4) after temperature jumping from 20 to 45 °C: 100 (■), 95 (▲), 90 (▼), 80 (◆), 70 (●), 60 (□), 40 (△), 20 (▽). The solid and dashed lines serve to connect the data, and the error bars, which are smaller than the symbols employed here, denote the standard error ($N = 3$).

despite dehydration with a higher NaCl concentration. This result suggests that even though a high content of SF can interrupt the phase transition by increased topological constraints, PN/SF IPNs keep the salt-responsive phase transition behavior of PNIPAAm without disrupting the conformational change related to the salt concentration.

Deswelling Kinetics of IPN Hydrogels. Figure 7 exhibits the deswelling kinetics of PN/SF (a) and PNA/SF (b) IPN hydrogels after the hydrogels swollen in the equilibrium state at 20 °C, below the T_p, were moved to the PBS bath at 45 °C, above the T_p. The swelling degree of the PN/SF100 hydrogel decreases very slowly to reach a new equilibrium. The clear and transparent PN/SF100 hydrogel swollen at 20 °C changed its appearance to opaque, and its smooth skin at 20 °C became hardened and rough at 45 °C. This indicates that PN/SF100 hydrogels show pronounced skin layer formation, which blocks the water flow from the hydrogel despite the gradually increased hydrodynamic internal pressure.[9]

In the deswelling process of the IPN hydrogels, we suppose three factors to control the deswelling kinetics: the skin layer formation, the aggregation force of PNIPAAm chains, and the physical restriction of SF networks that would act as a restraint against the volume change of the IPN networks. In Figure 7a, PN/SF95 does not show a significant difference from PN/SF100 in the deswelling curve, indicating that only 5 wt % SF networks is not enough to remove skin layer formation. However, the deswelling process becomes faster in the PN/SF IPN hydrogels containing more than 10 wt % SF. However, the transparent PN/SF90 hydrogel at 20 °C changed to opaque at 45 °C, which means that it still shows a weak skin layer formation. PN/SF80, PN/SF70, and PN/SF60, which did not become opaque but translucent at 45 °C, show faster deswelling kinetics than PN/SF100, PN/SF95, and PN/SF90. Even though PN/SF70 has more physical restriction by SF networks than PN/SF95 and PN/SF90, the decrease of the skin layer effect in PN/SF70 should overwhelm the physical restriction of SF networks in PN/SF70. However, PN/

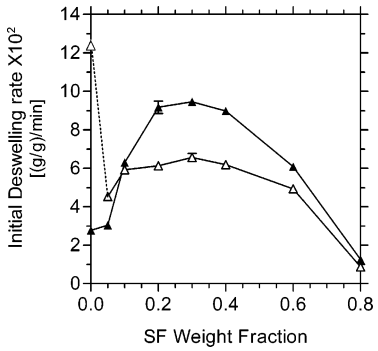

Figure 8. Initial deswelling rates of PN/SF (▲) and PNA/SF (△) IPN hydrogels calculated from the experimental conditions described in the text. The solid and dashed lines serve to connect the data, and the error bars, which are smaller than the symbols employed here, denote the standard error ($N = 3$).

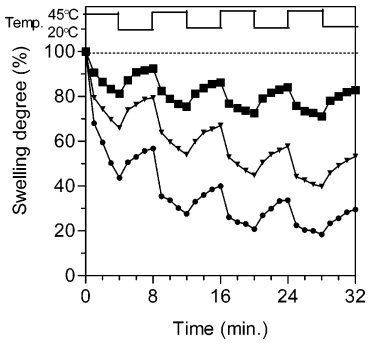

Figure 9. Oscillating swelling/deswelling properties of PN/SF100 (■), PN/SF90 (▼), and PN/SF70 (●) over 4 min cycles between 20 and 45 °C.

SF40 and PN/SF20 show decreased deswelling kinetics, because the restriction of SF networks might exceed the aggregation force of the PNIPAAm chains at a higher SF content.

In Figure 7b, the PNA/SF100 hydrogels show very fast deswelling kinetics upon increasing the temperature above the T_p. This suggests that the PNA/SF100 hydrogel does not show skin layer formation in the deswelling process. Incorporation of a hydrophilic moiety such as AAc into the PNIPAAm backbone should disrupt the skin layer structure observed in PN/SF100 hydrogels. However, PNA/SF IPNs show decreased deswelling kinetics, compared with the PNA/SF100 hydrogel. Three factors, the skin layer formation, the restriction of SF networks, and the aggregation force of the PNIPAAm chains, are here suggested to control the deswelling process in PNA/SF IPNs. The first factor, skin layer formation, should not be a major factor to control the deswelling process in PNA/SF IPNs, because P(NIPAAm-*co*-AAc) networks themselves do not have a significant skin layer. Therefore, the restriction of SF networks should operate as a major factor governing the deswelling process of PNA/SF IPN hydrogels, resulting in lower deswelling kinetics of PNA/SF IPNs than PNA/SF100.

The initial deswelling rates of PN/SF and PNA/SF IPN hydrogels are shown in Figure 8. The initial swelling rate was calculated from the decreased gel weight within 5 min after the gels were transferred to 45 °C per the swollen gel weight at 20 °C. At the curve for PN/SF IPN hydrogels, a maximum is shown at PN/SF70, but PN/SF80, PN/SF70, and PN/SF60 exhibit very similar initial swelling rates.

The SF networks not only increase the viscoelastic properties of PNIPAAm hydrogels, but also enhance their deswelling rates. The SF β sheet crystalline networks should act as drain channels for water molecules, so the increased hydrodynamic internal pressure at higher temperature drives internal water to be quickly expelled without significant blocking.

On the other hand, it is surprising that the initial deswelling rate curve of the PNA/SF IPNs shows a maximum peak at PNA/SF70 even though the peak of the PNA/SF IPNs is not as notable as the peak of the PN/SF IPNs. This means that the first factor still could control the deswelling kinetics in the PNA/SF IPNs: a weak skin layer effect remains in the PNA/SF IPN hydrogels. The fact that PNA/SF95 shows a lower initial deswelling rate than PNA/SF70 suggests the following: only 5 wt % SF networks disrupt the aggregation force of P(NIPAAm-*co*-AAc) chains in PNA/SF IPNs, similar to 30 wt % SF networks, and the 30 wt % SF networks reduce skin layer formation more effectively than do the 5 wt % SF networks. This result matches that of PN/SF95, which showed skin layer formation like PN/SF100, which means 5 wt % SF is not sufficient to prevent the skin layer effect in both PN/SF and PNA/SF IPNs. PNA/SF40 and PNA/SF20 exhibit decreased initial deswelling rates on a relatively large scale, indicating that the aggregation force of the NIPAAm-*co*-AAc chains competes with the physical restriction force of the SF networks, as shown in PN/SF40 and PN/SF20.

When the deswelling rates of PNA/SF IPNs are compared with those of PN/SF IPNs, we observe the effect of the AAc components on the aggregation force of the PNIPAAm networks without consideration of the skin layer effect. The skin layer effect is probably suppressed by the SF within these IPNs. Only PNA/SF95 shows a faster deswelling rate than PN/SF95 because of more skin layer formation in PN/SF95 than PNA/SF95. However, other PN/SF IPN hydrogels exhibit a faster deswelling rate than PNA/SF IPN hydrogels at other compositions except 5 wt % SF, indicating that the AAc component decreases the aggregation force of the PNIPAAm chains, when the skin layer effect is not considerable. Especially PN/SF70 and PNA/SF70 show the biggest difference between their initial deswelling rates: PNA/SF70 exhibits a 31% decrease of the initial deswelling rate, compared with PN/SF70. If it is considered that both PN/SF70 and PNA/SF70 should have low skin layer formation by well-developed SF network channels and the same physical restriction force of SF networks due to the same content of SF, their deswelling kinetics differences should be explained by the remaining factor, the aggregation force of PNIPAAm (or P(NIPAAm-*co*-AAc)). The strong hydrophobic aggregation force of the PNIPAAm backbone should be weakened due to the division of the PNIPAAm long chains into short sequences by incorporation of hydrophilic AAc units.[17] Therefore, if the skin layer effect is not considerable, incorporation of an AAc moiety should negatively affect the deswelling process, leading to a decrease of the deswelling rate.

Cyclic Swelling/Deswelling Properties. In actual applications of stimulus-responsive hydrogels to function as actuators regulating drug release or controlling artificial muscles, rapidly oscillating properties in response to a stimulus change are critically demanded. From the dynamic swelling and deswelling investigations, it was observed that the SF β sheet networks in the PN/SF IPNs improved the deswelling rate without a decrease of the swelling rate. Here, the swelling/deswelling properties of the PN/SF IPN hydrogels in response to short-term temperature cycles below and above the T_p are described.

The cyclic swelling/deswelling properties of PN/SF100, PN/SF90, and PN/SF70 were measured, and the results are represented in Figure 9. PN/SF IPN hydrogels are swollen until the equilibrium state in PBS at 20 °C and then placed into PBS at 45 °C. The hydrogels are then transferred back and forth over

4 min cycles. PN/SF100 hydrogels show a small decrease of weight in every deswelling cycle, resulting in no significant decrease of the swelling degree over repeated temperature jumping cycles. The swelling degree of PN/SF100 oscillates between 85% and 75% from the second cycle. This indicates that, in short temperature cycles, the deswelling rate of PN/SF100 is similar to its swelling rate. However, PN/SF90 and PN/SF70 exhibit more rapid decreases of the swelling degree in the deswelling process than PN/SF100 in every cycle. The oscillating curves of PN/SF90 and PN/SF70 gradually decrease.

The gradual decrease of the swelling degree of PN/SF90 and PN/SF70 can be explained in terms of their swelling rates not being as fast as their deswelling rates. PN/SF70 shows a faster decrease of the swelling degree than PN/SF90 in every cycle, indicating a faster deswelling rate. Even though the IPN hydrogels show a faster response in every deswelling cycle, their swelling process is not notably different from that of PN/SF100. This result shows that, in every temperature cycle, the SF networks accelerate the deswelling process by decreasing the skin layer effect and do not interrupt the swelling rate of the PNIPAAm networks.

Conclusions

In this study, we introduced novel protein/synthetic polymer hybrid hydrogels as interpenetrating networks of PNIPAAm with SF β sheet structure and investigated the effect of SF networks on the characteristics of PNIPAAm and PNIPAAm-*co*-AAc hydrogels. The IPN hydrogels show the same volume phase transition behavior responding to the temperature and salt concentration as PN/SF100 or PNA/SF100 and keep the swelling kinetics of PN/SF100 or PNA/SF100. This means that the SF β sheet networks interfere little, if any, with the volume phase transition of the PNIPAAm networks. The PN/SF IPNs with the β sheet crystalline structure of SF improved the viscoelastic properties, which was driven with more SF content. We investigated and compared the deswelling behaviors of PN/SF IPNs with those of PNA/SF IPNs. With the SF β sheet networks, the PN/SF IPNs show increased deswelling kinetics and exhibit a maximum rate at PN/SF70. This result indicates that the water molecules are rapidly released with reduced skin layer effects by more SF content, while the aggregation force of the PNIPAAm chains competes with the restriction of the SF networks.

From the above experiments, we can conclude that there are three parameters affecting the deswelling kinetics of the PN/SF: (1) skin layer formation, (2) restriction of SF β sheet networks, (3) aggregation force of the PNIPAAm networks. First, the skin layer formation in the deswelling process decreased with the incorporation of an AAc moiety and with more SF networks that act as water-draining channels. Second, the restriction effect of the SF β sheet networks increased with a higher SF content. Third, the aggregation force of the PNIPAAm networks decreased with the incorporation of an AAc moiety and with more SF content.

In the PN/SF IPNs, the overwhelming parameter was skin layer formation. The more SF β sheet networks the PN/SF IPNs contained, the less formation of a skin layer they showed, resulting in the increased deswelling rate. When the SF β sheet networks significantly decreased the skin layer formation in PN/SF IPNs, the restriction force of the SF β sheet networks competed with the aggregation force of the PNIPAAm networks, showing a maximum deswelling rate at 30 wt % SF content.

PNA/SF IPNs showed a very low influence of skin layer formation, because P(NIPAAm-*co*-AAc) networks originally do not have significant skin layer formation. Therefore, in PNA/SF IPNs, the restriction force of the SF β sheet networks competes with the aggregation force of the P(NIPAAm-co-AAc) networks weakened by incorporation of AAc, exhibiting lower deswelling rates than PN/SF IPNs. However, there exist skin layer effects even in PNA/SF IPNs, which decrease with more SF networks, showing a weak maximum among their deswelling rates at PNA70.

Acknowledgment. This work was supported by Nexia Biotechnologies Inc. (Vaudreuil-Dorion, Quebec, Canada).

References and Notes

(1) Gupta, P.; Vermani, K.; Garg, S. *Drug Discovery Today* **2002**, *7*, 569.
(2) Yokoyama, M. *Drug Discovery Today* **2002**, *7*, 426.
(3) Chilkoti, A.; Dreher, M. R.; Meyer, D. E.; Raucher, D. *Adv. Drug Delivery Rev.* **2002**, *54*, 613.
(4) Galaev, L. Y.; Mattiasson, B. *Trends Biotechnol.* **2000**, *17*, 335.
(5) Sharma, S.; Kaur, P.; Jain, A.; Rajeswari, M. R.; Gupta, M. N. *Biomacromolecules* **2003**, *4*, 330.
(6) Gil, E. S.; Hudson, S. M. *Prog. Polym. Sci.* **2004**, *29*, 1173.
(7) Diez-Pena, E.; Quijada-Garrido, I.; Barrales-Rienda, J. M. *Polymer* **2002**, *43*, 4341.
(8) Varga, I.; Gilanyi, T.; Meszaros, R.; Filipcsei, G.; Zrinyi, M. *J. Phys. Chem. B* **2001**, *105*, 9071.
(9) Yoshida, R.; Uchida, K.; Kaneko, Y.; Sakai, K.; Kikuchi, A.; Sakurai, Y.; Okano, T. *Nature* **1995**, *374*, 240.
(10) Jeong, B.; Lee, K. M.; Gutowska, A.; An, Y. H. *Biomacromolecules* **2002**, *3*, 865.
(11) Jeong, B.; Bae, Y. H.; Lee, D. S.; Kim, S. W. *Nature* **1997**, *388*, 860.
(12) Chung, J. E.; Yokoyama, M.; Aoyagi, T.; Sakurai, Y.; Okano, T. *J. Controlled Release* **1998**, *53*, 119.
(13) Magoshi, T.; Ziani-Cherif, H.; Ohya, S.; Nakayama, Y.; Matsuda, T. *Langmuir* **2002**, *18*, 4862.
(14) Nath, N.; Chilkoti, A. *J. Am. Chem. Soc.* **2001**, *123*, 8197.
(15) Benns, J. M.; Choi, J.; Mahato, R. I.; Park, J.; Kim, S. W. *Bioconjugate Chem.* **2000**, *11*, 637.
(16) Schild, H. G. *Prog. Polym. Sci.* **1992**, *17*, 163.
(17) Kaneko, Y.; Nakamura, S.; Sakai, K.; Aoyagi, T.; Kikuchi, A.; Sakurai, Y.; Okano, T. *Macromolecules* **1998**, *31*, 6099.
(18) Annaka, M.; Sugiyama, M.; Kasai, M.; Nakahira, T.; Matsuura, T.; Seki, H.; Aoyagi, T.; Okano, T. *Langmuir* **2002**, *18*, 7377.
(19) Liu, L.; Sheardown, H. *Biomaterials* **2005**, *26*, 233.
(20) Dhara, D.; Rathna, G. V. N.; Chatterji, P. R. *Langmuir* **2000**, *16*, 2424.
(21) Beebe, D. J.; Moore, J. S.; Bauer, J. M.; Qing, Y. Q.; Robin, H.; Liu, R. H.; Chelladurai, D. C.; Jo, B. *Nature* **2000**, *404*, 588.
(22) Zhang, X.; Wu, D.; Chu, C. *Biomaterials* **2004**, *25*, 3793.
(23) Zhou, C. Z.; Confalonieri, F.; Medina, N.; Zivanovic, Y.; Esnault, C.; Yang, T.; Jacquet, M.; Janin, J.; Duguet, M.; Perasso, R.; Li, Z. G. *Nucleic Acids Res.* **2000**, *28*, 2413.
(24) Jin, H.; Kaplan, D. L. *Nature* **2003**, *424*, 1057,
(25) Ha, S.; Park, Y. H.; Hudson, M. S. *Biomacromolecules* **2003**, *4*, 488.
(26) Nazarov, R.; Jin, H.; Kaplan, D. *Biomacromolecules* **2004**, *5*, 718.
(27) Gotoh, Y.; Tsukada, M.; Minoura, N.; Imai, Y. *Biomaterials* **1997**, *18*, 267.
(28) Minoura, N.; Tsukada, M.; Nagura, M. *Polymer* **1990**, *31*, 265.
(29) Gu, J.; Yang, X.; Zhu, H. *Mater. Sci. Eng., C* **2002**, *20*, 199.
(30) Gil, E. S.; Spontak, R. J.; Hudson, S. M. *Biomacromol. Sci.* **2005**, *5*, 702.
(31) Gil, E. S.; Frankowski, D. J.; Spontak, R. J.; Hudson S. M. *Biomacromolecules* **2005**, *6*, 3079.
(32) Gil, E. S.; Frankowski, D. J.; Bowman M. K., Gozen A. O.; Hudson S. M.; Spontak, R. J.; *Biomacromolecules* **2006**, *7*, 728.
(33) Shibayama, M.; Tanaka, T. *Adv. Polym. Sci.* **1993**, *109*, 1.
(34) Hoffman, A. S.; et al. *J. Biomed. Mater. Res.* **2000**, *52*, 577.
(35) Lee, A. S.; Butun, V.; Vamvakaki, M.; Armes, S. P.; Pople, J. A.; Gast, A. P. *Macromolecules* **2002**, *35*, 8540.
(36) Park, T. G.; Hoffman, A. S. *Macromolecules* **1993**, *26*, 5045.

BM060543M